Environmental Science & Technology

Article

pubs.acs.org/est

Effect of Chloride on the Dissolution Rate of Silver Nanoparticles and Toxicity to *E. coli*

Clément Levard,*[,†,‡,#] Sumit Mitra,[†] Tiffany Yang,[†] Adam D. Jew,[†] Appala Raju Badireddy,[‡,§] Gregory V. Lowry,[‡,∥] and Gordon E. Brown, Jr.[†,‡,⊥]

[†]Surface and Aqueous Geochemistry Group, Department of Geological & Environmental Sciences, Stanford University, Stanford, California 94305-2115, United States

[‡]Center for Environmental Implications of NanoTechnology (CEINT), Duke University, Durham, North Carolina 27708-0287, United States

[§]Department of Civil and Environmental Engineering, Duke University, Durham, North Carolina 27708, United States

[∥]Department of Civil and Environmental Engineering, Carnegie Mellon University, Pittsburgh, Pennsylvania 15213, United States .

[⊥]Department of Photon Science and Stanford Synchrotron Radiation Lightsource, SLAC National Accelerator Laboratory, 2575 Sand Hill Road, Menlo Park, California 94025, United States

Supporting Information

ABSTRACT: Pristine silver nanoparticles (AgNPs) are not chemically stable in the environment and react strongly with inorganic ligands such as sulfide and chloride once the silver is oxidized. Understanding the environmental transformations of AgNPs in the presence of specific inorganic ligands is crucial to determining their fate and toxicity in the environment. Chloride (Cl^-) is a ubiquitous ligand with a strong affinity for oxidized silver and is often present in natural waters and in bacterial growth media. Though chloride can strongly affect toxicity results for AgNPs, their interaction is rarely considered and is challenging to study because of the numerous soluble and solid Ag–Cl species that can form depending on the Cl/Ag ratio. Consequently, little is known about the stability and dissolution kinetics of AgNPs in the presence of chloride ions. Our study focuses on the dissolution behavior of AgNPs in chloride-containing systems and also investigates the effect of chloride on the growth inhibition of *E.coli* (ATCC strain 33876) caused by Ag toxicity. Our results suggest that the kinetics of dissolution are strongly dependent on the Cl/Ag ratio and can be interpreted using the thermodynamically expected speciation of Ag in the presence of chloride. We also show that the toxicity of AgNPs to *E.coli* at various Cl^- concentrations is governed by the amount of dissolved $AgCl_x^{(x-1)-}$ species suggesting an ion effect rather than a nanoparticle effect.

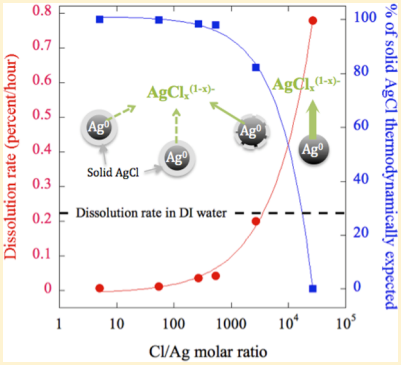

INTRODUCTION

Silver nanoparticles (AgNPs) are among the most widely used types of NPs in consumer products and have been shown to be a potenital threat to the environment.[1−6] Because of their antibacterial, antiviral, and antifungal properties, AgNPs and released Ag^+ ions have been found to be highly toxic to a variety of organisms.[1−6] Regrettably, many of the toxicity studies that have been conducted with AgNPs are not environmentally relevant because they do not consider the transformations these nanoparticles undergo in various environments.[7] After AgNPs have been released into the environment, their composition, structure, and surface properties are altered, resulting in a change of their physicochemical properties.[8−10] Therefore, the environmental transformations of AgNPs need to be investigated to determine the changes in their surface properties and reactivity (e.g., dissolution), which in turn will affect their transport, reactivity, and toxicity to organisms in soils and natural waters.[7,8,11] On the basis of simple equilibrium thermodynamic modeling, AgNPs, once oxidized, will mostly react with reduced sulfur groups and chloride (Cl^-) ions. In nature, the predominant species will depend on the redox state of the solution and the availability of each ligand.[7] It is important to note that the initial oxidation step of metallic silver to Ag(I) is a prerequisite before it can react with reduced sulfur and chloride. When exposed to oxygen, silver reacts to form a silver oxide (Ag_2O) surface layer. The oxidation of silver is thermodynamically favorable at room temperature.[12] In a reducing environment with available sulfide, Ag_2S is the predominant transformation product.[9,13,14] However, the nature of the oxidant has never been clearly identified in these cases. An important consequence of sulfidation is that it strongly decreases further oxidation of the AgNPs[10] and ion release, and therefore their toxicity to *Escherichia coli*.[11] Another important reaction to consider when assessing the behavior of AgNPs in the environment, particularly in oxic environments

Received: January 25, 2013
Revised: April 19, 2013
Accepted: May 3, 2013
Published: May 3, 2013

where the amount of sulfide is low, is how they react with Cl^- ions. Besides being one of the most prevalent monovalent anions in natural aqueous systems, Cl^- is present in most growth media used for testing the toxicity of AgNPs to organisms. Although the interaction between Cl^- and Ag^+ ions and the effect of Cl^- on Ag^+ ion toxicity have been studied extensively,[15−17] the effect of Cl^- on the stability of AgNPs has been explored in only a few studies. In one such study, Li et al. showed that the stability of AgNPs is strongly affected by the presence of Cl^-, with formation of a AgCl layer on the AgNPs that inhibits their dissolution at a low Cl/Ag ratio.[18] In another study, Ho et al. showed that at low Cl/Ag ratio, the presence of Cl^- ions in solution can completely inhibit or significantly decrease the rate of Ag-NPs dissolution in the presence of a strong oxidant.[19] A high Cl/Ag ratio, however, may enhance dissolution due to the formation of soluble $AgCl_x^{(x-1)-}$ species. Because Ag toxicity is often governed by the amount of dissolved Ag in solution, it has been proposed that Cl^- will have a strong effect on the toxicity of AgNPs. A good example is a study by Gupta et al. who looked at the effect of chloride, bromide, and iodide on the toxicity of $AgNO_3$ to *E. coli*.[17] These authors hypothesized that at low Cl/Ag ratios, Ag^+ ions precipitate with Cl^- to form solid AgCl, whereas at higher Cl/Ag, there is an increase of soluble $AgCl_x^{(x-1)-}$ species, resulting in decreased Ag resistance by *E. coli*. Although Cl^- interactions with dissolved Ag^+ have been studied, little is known about the kinetics of AgNP dissolution and the resulting toxicity as a function of Cl/Ag ratio.

The focus of this study is on determining the rates of dissolution of polyvinylpyrrolidone-coated AgNPs at different Cl/Ag ratios (total Cl concentration vs total Ag concentration in suspension) and understanding the toxicity of Ag-NPs at various concentrations on *E. coli* (ATCC strain 33876) as a function of chloride concentrations that mimic natural conditions (0.5, 0.1, and 0.01 M NaCl and DI water). By varying the Cl/Ag ratio in solution, we hypothesize that the rate of dissolution of AgNPs and the resultant toxicity will be strongly correlated with the speciation of Ag in the presence of chloride.

MATERIALS AND METHODS

PVP-Coated AgNPs Synthesis. AgNPs were synthesized following a protocol adapted from Kim et al.[20] First, 13.5 g of polyvinylpyrrolidone (PVP, Sigma-Aldrich, $M_{w(ave)}$ = 10 000 Da, CAS Number 9003-39-8) was dissolved in 50 mL of ethylene glycol. After heating the solution to 140 °C, 3.15 g of $AgNO_3$ (Sigma-Aldrich) in deionized (DI) water (3 mL) was added to the ethylene glycol and reacted for 2 h. The solution was then cooled to 25 °C, and the AgNPs were separated from the ethylene glycol using 100% acetone (100 mL) followed by centrifugation at a relative centrifugal force maximum value (RCF_{max}) of 26,040*g* for 1 h. A final washing procedure was carried out twice in which the particles were washed with DI water and centrifuged again for 1 h.

SEM and Zeta Potential Measurements. Size distribution and shape of the AgNPs were determined by scanning electron microscopy (SEM). AgNP samples in aqueous solution were deposited on a silicon wafer and dried in air. SEM images of the initial AgNPs were collected with a FEI-XL30 Sirion SEM (accelerating voltage of 5 kV). The electrophoretic mobility was measured using a Malvern ZetaSizer NanoSeries at pH 7.2 ± 0.2 in both 0.01 M $NaNO_3$ and 0.01 M NaCl and converted to ζ potential using the Henry's equation.

AgNP Dissolution Rates in the Presence of Chloride. Experiments to determine the rates of dissolution of the AgNPs in solutions with different salt concentrations were carried out in Float-A-Lyzer G2 dialysis devices with a membrane with a nominal molar mass cutoff of 8−10 kDa. To ensure that Ag^+ ions were not lost by adsorption to the dialysis membrane, a control experiment using 1.10^{-4} and 1.10^{-5} M $AgNO_3$ in DI water was performed with recoveries of 97.2% and 96.9%, respectively. Diffusion of Ag^+ ions through the dialysis membrane was fast relative to the measured Ag NP dissolution rates and did not significantly affect the dissolution rate measurements. Aqueous solutions containing 2.10^{-3}, 2.10^{-4}, 2.10^{-5}, and 2.10^{-6} M of AgNPs were made from the stock solution by dilution with DI water. Each of these solutions was divided into four vials, and NaCl was added to provide salt concentrations of 0, 0.01, 0.1, and 0.5 M in 5 mM HEPES buffer (to control pH). Each experiment was performed in duplicate, which resulted in a total of 32 reaction vessels. Eight milliliters of a AgNP/NaCl suspension was added to each dialysis tube, and 25.0 ± 0.1 mL of the corresponding DI or NaCl solutions was added to the outer vial. The solution in the outer vial was replaced with fresh NaCl solution every 2 h for 36 h to maintain the maximum driving force for dissolution of the particles. The removed solution was acidified in HNO_3 (70%) for 1 h and diluted to 5% HNO_3 to measure the dissolved Ag species with an inductively coupled plasma-atomic emission spectrometer (ICP-AES) spectrometer (TJA IRIS Advantage/1000 Radial ICAP spectrometer). The pH of the Ag-containing solutions was measured prior to and after each experiment and found to be 7.2 ± 0.2.

AgNP-Aged Solutions for Growth Inhibition Experiments on *E. coli*. *E. coli* was exposed to Ag NPs that had been aged in media with different chloride content for 12 d. So in parallel, a series of AgNPs were aged for 12 days in solutions with the same NaCl concentrations as those used in the dissolution rate studies (detailed above). AgNP solutions were made by diluting the stock solution in DI water to 2.10^{-3}, 2.10^{-4}, 2.10^{-5}, and 2.10^{-6} M. To confirm the total Ag concentrations, aliquots were dissolved in HNO_3 (70%) for 1 h and diluted to 5% HNO_3 and analyzed using ICP-AES. As in the dissolution rate study, each suspension was divided into four aliquots, and NaCl was added to provide a salt concentration of 0, 0.01, 0.1, or 0.5 M NaCl. These suspensions were placed on an orbital shaker (100 rpm/min) for 12 days in the dark in air-saturated solutions (8.6 mg/L DO) at room temperature. The total soluble Ag species for each NaCl concentration was measured after 12 days of aging. Particles were separated from the solution using Amicon ultra centrifugal filters (NMWL 3 kDa) at 6000*g* (RCF_{max}) for 20 min. The 3 kDa nominal molecular weight cutoff was sufficient to separate AgNPs from Ag^+ ions. In control experiments performed as part of a previous study, it was demonstrated that silver ions (added as $AgNO_3$ at 0.1 to 1 mg/L) were 100% recovered, indicating that loss of Ag^+ ions to the filters was negligible.[21] The amount of soluble Ag species was measured using ICP-AES. Three replicates of each sample were analyzed.

***E. coli* Growth Inhibition Tests.** The effect of aging AgNPs in Cl-rich aqueous solutions on the growth rate of *E. coli* (ATCC strain 33876) was determined by exposing *E. coli* to AgNPs in solutions containing different concentrations of Cl^- and measuring optical densities by UV−vis absorption at λ =

dx.doi.org/10.1021/es400396f | Environ. Sci. Technol. 2013, 47, 5738−5745

600 nm (OD_{600}). The growth inhibition was calculated by converting the OD_{600} into colony-forming units (CFU) using a calibration curve created with an *E. coli* control that did not have any AgNPs (see the Supporting Information for details).

E. coli were first inoculated in Luria−Bertani (LB) medium (10 g tryptone, 5 g yeast extract, and 5 g NaCl (0.085 M chloride) for 1 L of medium) and incubated for 16 h at 37 °C on an orbital shaker (150 rpm). At the same time, four reaction vessels were filled with LB media containing 0, 0.01, 0.1, and 0.5 M NaCl, which were the same NaCl concentrations as those used in the AgNP aging experiments. After 16 h, the *E. coli* stock solution was split into four vessels to wash the cells. Each vessel was centrifuged to form a pellet. The pellet was resuspended in DI water, then centrifuged again. The supernatant was discarded, and the resulting pellets were resuspended in their respective media. The *E. coli* solutions were then diluted to ∼1 to 2 × 10^7 CFU/mL (OD_{600} of 0.02). Then, 0.75 mL aliquots of the aged (12 d) particles were added to 0.75 mL of *E. coli* resuspended in their respective media. The resulting solutions were vortexed for 10 s and incubated at 37 °C for 24 h on an orbital shaker (150 rpm). After 24 h, OD_{600} was measured and converted to CFU/mL using the calibration curve. Control experiments without AgNPs were performed under the same conditions. A PVP control experiment has also been done to test an eventual toxicity of the coating (10 mg/L) and did not show any effect on growth. The same experiment was also conducted to determine the effect of Ag^+ only (as $AgNO_3$ in DI water) on *E. coli* growth inhibition. All experiments were performed in triplicate under sterile conditions.

RESULTS AND DISCUSSION

Properties of AgNPs. The synthesized nanoparticles were characterized by SEM before adding chloride and were found to be relatively monodispersive in size with an average diameter of 32.9 nm ± 4.9 nm (Figure 1). The zeta potential measured at pH 7.2 ± 0.2 in 0.01 M $NaNO_3$ was found to be −8.8 mV. The observed negatively charged surface at neutral pH is consistent with previous zeta potential measurements performed on PVP-coated AgNPs.[10,22,23]

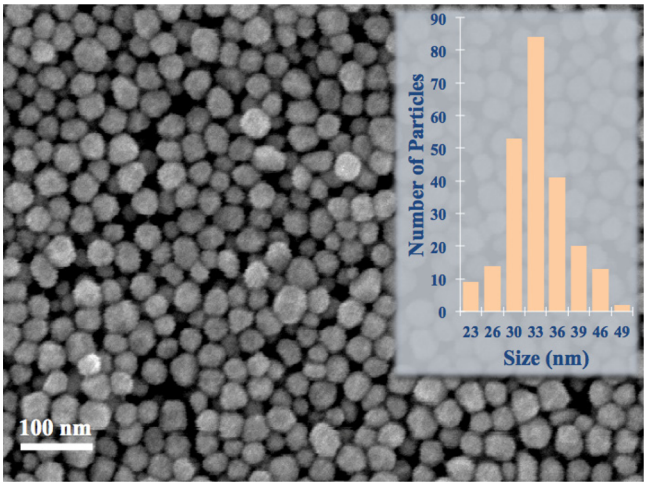

Figure 1. SEM image of the initial unreacted AgNPs. Size distribution shown in the inset was obtained by measuring 250 particles in two different SEM images.

Rates of AgNP Dissolution in Presence of Different Chloride Concentrations. The percentage of soluble Ag species released over time for different Cl/Ag ratios (normalized by the total amount of Ag to account for small variations in the initial Ag NP concentration) are shown in Figure 2. A small amount of chloride significantly decreases the rate of release of soluble Ag species compared to the chloride-free control (labeled DI water in Figure 2). Furthermore, the initial rate of aqueous Ag release ($t \leq 10$ h) into solution increased as the Cl/Ag molar ratio increased from 5 to 26750 (Figure 2 and Table 1). The differences in release behavior are discussed later in the paper.

For Cl/Ag ≤ 2675, the rate of dissolution of the AgNPs in the presence of chloride was slower compared to AgNPs in DI water, but for a high Cl/Ag ratio (Cl/Ag = 26750), the rate of AgNP dissolution is greater than the DI water control. The nature of the soluble Ag species that forms in solution varies as a function of total Ag and Cl^- concentration and include Ag^+, $AgCl_{aq}$, $AgCl_2^-$, $AgCl_3^{2-}$, and $AgCl_4^{3-}$ as predicted by thermodynamics (Figure 3), where the experimental conditions tested in this study are represented as red dots. This predominance diagram indicates that, generally, as the Cl/Ag ratio increases, $AgCl_x^{(x-1)-}$ soluble species begin to dominate compared to solid AgCl. This was seen in the Cl/Ag ≥ 26750 reaction vessel in which solid AgCl is predicted to be thermodynamically unstable. Thermodynamic calculations for this particular experiment ([AgNPs] = 2.10^{-5} M, [NaCl] = 0.5M) indicate the following Ag speciation: $AgCl_2^-$ (51%), $AgCl_3^{2-}$ (27%), and $AgCl_4^{3-}$ (22%). For all other experimental conditions (Cl/Ag ≤ 2675), solid AgCl is expected to be the dominant phase. These results suggest that the rate of dissolution is strongly dependent on the solid AgCl/$AgCl_x^{(x-1)-}$ ratio, with AgNP dissolution rate increasing as solid AgCl/$AgCl_x^{(x-1)-}$ decreases.

Zeta potential measurements for samples in either 0.01 M $NaNO_3$ or 0.01 M NaCl electrolyte solutions were measured and suggest that the AgNPs are covered with AgCl. Because pure AgCl particles have high negative zeta potentials (−57 mV),[23] any significant variation in zeta potential after addition of chloride to samples with a nonbimodal distribution of zeta potentials would indicate that the AgNPs are coated with AgCl. In 0.01 M $NaNO_3$ solutions, the zeta potential was found to be −8.8 mV with a monomodal distribution of the charge with a peak width of 9.6 mV. The same measurement performed in a 0.01 M NaCl solution resulted in a zeta potential of −28.4 mV, again with a monomodal distribution and a peak width of 9.7 mV. The same trend was observed in 0.1 M $NaNO_3$ and NaCl (data not shown). These zeta potentials are similar to those measured in previous studies and support the hypothesis that the AgNPs are coated with AgCl. This AgCl coating can be the result of direct precipitation of AgCl at the surface of the oxidized AgNPs forming a more or less uniform layer but can also be the result of the sorption of small AgCl nucleates that first form in solution. The growth mechanism of an AgCl structure on the surface of the AgNPs is difficult to characterize on nanoparticles; however, such processes have been studied on silver substrates in a chloride-rich environment. In a recent study, AgCl particles were found to nucleate on scratches present on the surface of Ag wires (0.5 mm in diameter), which are favorable sites for heterogeneous nucleation.[25] The nuclei were found to expand laterally on the substrate until they formed a continuous film. Ionic transport through the newly formed continuous AgCl film was via the spaces between the

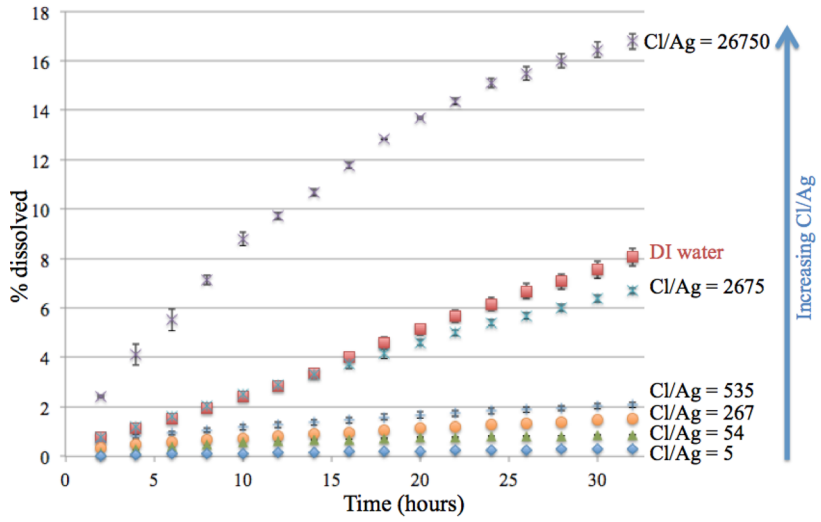

Figure 2. Percent of nanoparticulate silver dissolved over time for different Cl/Ag ratios compared with that of AgNPs in DI water. Each point represents the average of two experimental points. Extremities of the vertical bar on each point represent those two experimental points.

Table 1. Initial Dissolution Rates ($t \leq 10$ h) of AgNPs as a Function of Cl/Ag Ratio

Cl/Ag molar ratio	5	54	267	535	2675	26750
initial rate (%/hour) ± standard error	0.012 ± 0.001	0.056 ± 0.004	0.068 ± 0.011	0.107 ± 0.020	0.240 ± 0.013	0.850 ± 0.036

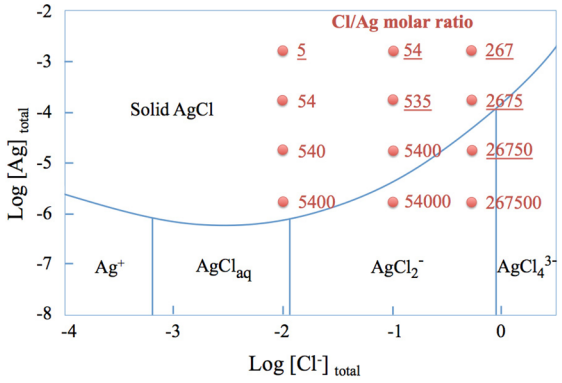

Figure 3. Predominance diagram for Ag^+ and $AgCl_x^{(x-1)-}$ species calculated using Medusa.[24] Experimental conditions with corresponding Cl/Ag molar ratios from this study are represented as red dots. The underlined ratios were the only ones that resulted in measurable releases of soluble silver species in the dissolution studies, and for the other conditions, the amount of soluble Ag species was below the detection limit of 1.8×10^{-8} mol/L.

AgCl grains. As the film thickened, the spaces between the AgCl grains were closed, and the ionic transport was mainly via microchannels running through the AgCl grains. The surfaces of nanoparticles are known to exhibit structural defects that might be favorable sites for nucleation of AgCl particles than can expand laterally to form more or less continuous AgCl films at the surface of the particles, slowing their dissolution rate. Similarly, Li et al. have shown that AgNPs aggregated in aqueous solution containing chloride and were encapsulated by a secondary phase that was attributed to the formation of AgCl precipitate at the surface of the AgNPs.[18]

The effects of both a AgCl surface precipitate/sorption and the formation of soluble $AgCl_x^{(x-1)-}$ species on the dissolution behavior of AgNPs were further investigated by closer inspection of the dissolution curves (Figure 4). The dissolution rates after 2 h of reaction time are reported in Table 1 and depend strongly on the Cl/Ag ratio as discussed previously (Table 1).

These results indicate that the reaction of AgNP surfaces with chloride ions (resulting in precipitation of solid AgCl or formation and diffusion of soluble $AgCl_x^{(x-1)-}$ species) occurs within the first 2 h. After 2 h, one can distinguish different stages in the dissolution behavior of the AgNPs for different Cl/Ag ratios (Figure 4). For a low Cl/Ag ratio (Cl/Ag $\leq$ 535) for which solid AgCl is expected to form, dissolution rate first exhibits a logarithmic/polynomial behavior (Figure 4, blue curves) that can be interpreted as a transient stage during which deposition of a solid AgCl layer (surface precipitation or sorption of small AgCl nucleates) on the AgNPs tends to reach a steady state between precipitation/sorption and dissolution. The duration of this transient stage decreases as the Cl/Ag ratio increases. This transient stage is not observed for the highest Cl/Ag ratio, which is consistent with the fact that solid AgCl is not expected to precipitate under these conditions. For these highest ratios, a linear trend (Figure 4, red lines) was observed and is attributed to the dissolution of the AgNPs. A third stage was observed only for the highest Cl/Ag ratio (Cl/Ag = 26750) after 10 h and 8% dissolution where the dissolution rate starts decreasing over time (Figure 4, green curve). One possible explanation for the dissolution behavior at a Cl/Ag of 26750 is that the first linear portion (up to about 8% dissolution) is driven by the formation of soluble Ag species, which cause the initial oxidized layer present on the surface of the AgNPs to dissolve relatively quickly compared to the dissolution rate in the DI water system. Even though they are hard to detect, thin layers of Ag_2O at the surface of AgNPs are thermodynamically expected in aerobic system and were detected in numerous studies using UV–vis spectroscopy.[12,26−28] The presence of an oxidized layer at the surface of the AgNPs synthesized for this study is indirectly shown by the nanoparticles dissolving in DI water over time. Studies in which this oxidized layer on the AgNP surfaces is absent (anaerobic conditions) have shown that the nanoparticles do not dissolve during the experimental

dx.doi.org/10.1021/es400396f | Environ. Sci. Technol. 2013, 47, 5738−5745

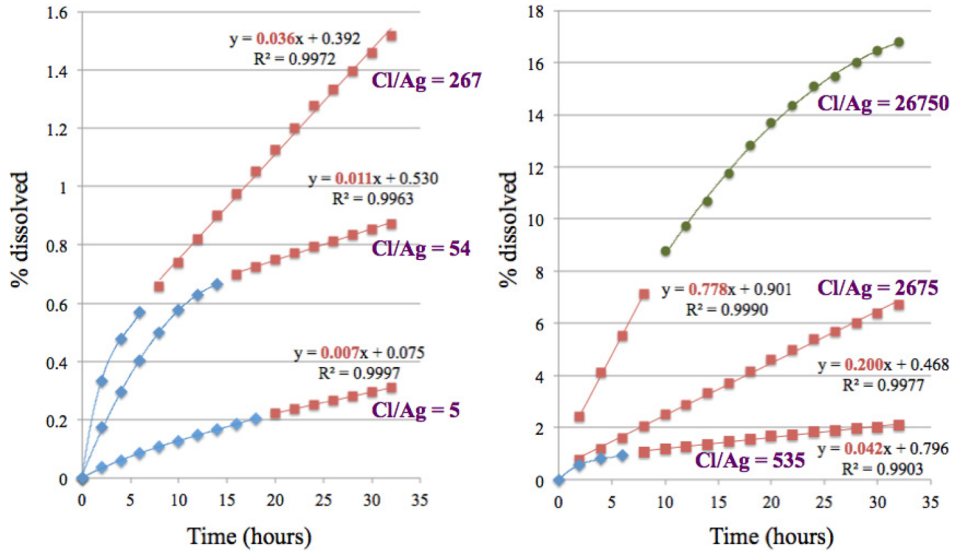

Figure 4. Dissolution of AgNPs for different Cl/Ag ratios. Experimental data (blue diamonds, red squares, and the green circles) are fit with a combination of polynomial (blue and green) and linear functions (red). The different colors represent different stages in the dissolution behavior of the AgNPs discussed in the text. The *y*-axis is a different scale for the two graphs.

time frame in DI water.[29] Once the oxidized surface layer is dissolved, the rate of dissolution might be partly or completely controlled by the oxidation reaction of the zerovalent AgNP surfaces. This oxidation step is most likely the kinetically limiting step for pure AgNP dissolution and explains the decrease in the dissolution rate above 8% dissolution. This process can be seen as an oxidation reaction in series with a ligand-assisted ion release from the oxide.

The dissolution rates of the AgNPs, determined from the slopes of the red line sections in Figure 4 are plotted as a function of the Cl/Ag ratio in Figure 5. The dissolution rate for

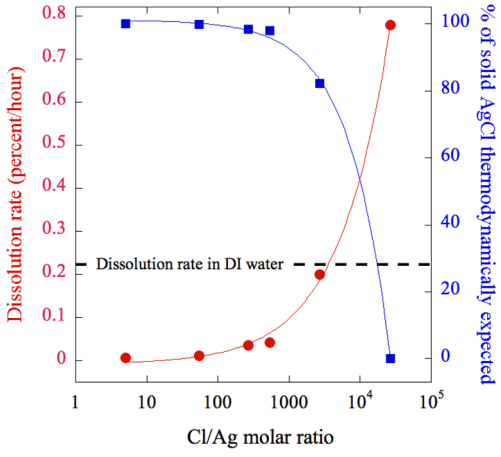

Figure 5. Dissolution rates of AgNPs as a function of Cl/Ag ratio (red circles) and the proportion of thermodynamically expected solid AgCl as a function of Cl/Ag ratio (blue squares). The dissolution rate of AgNPs in DI water is shown by a dashed line for comparison.

Cl/Ag = 5 is 36 times slower than for AgNPs in DI water. As the Cl/Ag ratio increases, the dissolution rates increase exponentially as the amount of thermodynamically expected solid AgCl decreases. For the highest Cl/Ag ratio (Cl/Ag = 26750), for which no solid AgCl is expected to form, the dissolution rate is 3 times higher than in DI water. This graph clearly shows the strong correlation between the kinetics of dissolution of the AgNPs and the expected speciation of Ag in presence of chloride ions. One could expect that aggregation will also affect the dissolution rate, especially for the high Cl concentration. Indeed, fast aggregation was observed for all the experiments performed in 0.5 M NaCl. In all other cases, the suspensions were stable over the course of the experiment (Figure S2, Supporting Information). However, dissolution rate better correlates with the Cl/Ag ratio (Figure 5) rather than the aggregation state of the particles (see the Supporting Information for more details).

Dissolution of AgNPs after 12 days. The amount of soluble Ag species after 12 days of mixing the AgNPs with different NaCl concentrations was measured (Figure 6). Overall, the amount of soluble Ag species present in solution when chloride is consistent with the thermodynamic prediction (dashed lines). However, the observed differences suggest that

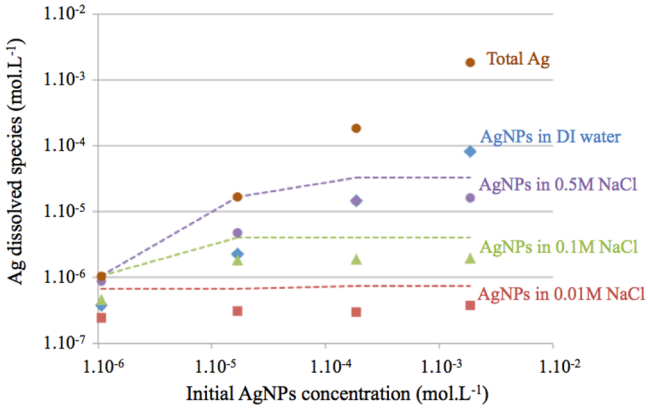

Figure 6. Soluble Ag species after 12 days of aging for different AgNPs initial concentrations (2.10^{-3}, 2.10^{-4}, 2.10^{-5}, and 2.10^{-6} M) and NaCl concentrations (0, 0.01, 0.1, and 0.5 M). The experimental data are represented by different symbols for the different NaCl concentrations (error bars are smaller than the symbols). The dashed lines represent the equilibrium thermodynamic predictions for the Ag–Cl systems. The total amount of Ag (AgNPs + soluble Ag species) for each initial concentration of AgNPs is also shown.

dx.doi.org/10.1021/es400396f | *Environ. Sci. Technol.* 2013, 47, 5738–5745

equilibrium (solubility) was not achieved after 12 days. Figure 6 shows that Cl^- has a strong effect on the solubility of the AgNPs.

Effect of Chloride on *E. coli* Growth Rates. The *E. coli* toxicity experiments were performed with the Ag nanoparticles that were aged for 12 days before exposure to the *E. coli* bacteria. This was done primarily because the amount of soluble Ag species, hypothesized to be the main toxic species (either Ag^+ or $AgCl_x^{(x-1)-}$ species), is controlled by the equilibrium thermodynamics of the Ag−Cl system (Figure 6). Therefore, it was possible to work with identical initial concentrations of soluble Ag species with different nanoparticle concentrations. As an example, the amount of dissolved Ag species for initial particle concentrations of 2×10^{-3}, 2×10^{-4}, and 2×10^{-5} M was relatively constant ($2 \times 10^{-6} \pm 9 \times 10^{-7}$ M) when aged in 0.1 M NaCl after 12 days (Figure 6). These systems are ideal to test whether the soluble Ag species or the AgNPs are responsible for Ag toxicity. This debate has been the focus of numerous studies that have attempted to determine the origin of AgNP toxicity.[30−35]

Figure 7 shows the inhibition in growth of *E. coli* as a function of Cl^- concentration after 24 h of exposure. The

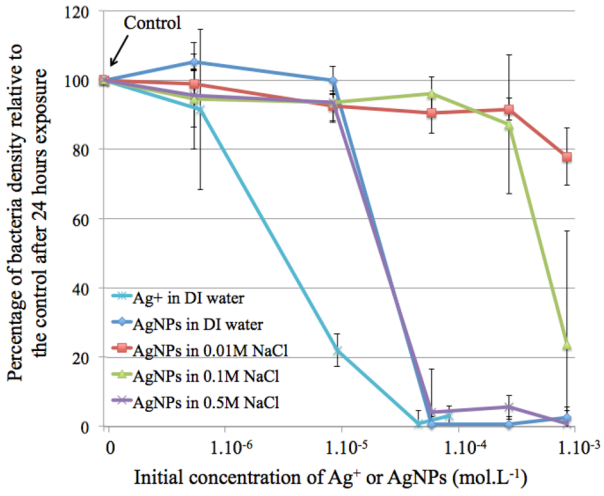

Figure 7. Percentage of bacterial density relative to the undosed control for the different AgNPs−Cl and Ag^+ systems after 24 h of exposure.

highest growth inhibition occurred for Ag^+ in DI water followed by AgNPs in DI water, 0.5 M NaCl, 0.1 M NaCl, and 0.01 M NaCl. The differences in growth rates as a function of Ag dosing are significant. Batch reactors containing AgNPs with no Cl^- or 0.5 M NaCl completely inhibited growth, whereas AgNPs aged in 0.01 M NaCl (primarily AgCl(s) expected) had little effect on growth rates. The effect of the toxicity experiment with AgNPs aged in a 0.1 M NaCl solution was between that of the two cases described above. These results are in good agreement with the dissolution data for the Ag nanoparticles just before they were introduced to the bacteria (Figure 6). Almost complete growth inhibition (<5% growth compared to the control experiment) was observed for all of the experiments that had a threshold of 3×10^{-6} M soluble Ag species (the original stock solution containing 6×10^{-6} M soluble Ag was diluted by a factor of 2 before being added to the bacteria). This result strongly suggests that Ag toxicity is due to exposure to soluble species of Ag rather than a Ag nanoparticle effect, which is consistent with most toxicity studies using microorganisms that report that dissolved Ag best explains the observed toxicity of AgNPs to bacteria. Xiu et al. has clearly shown that toxicity to *E. coli* is directly correlated with the amount of Ag^+ present in solution.[31] Our work demonstrates that the interactions of AgNPs and released Ag ions with inorganic ligands such as chloride must be considered in interpreting toxicity data.

It is also worth noting that the toxicity effects of the AgNPs in DI and in 0.5 M NaCl are similar. This is because similar amounts of soluble Ag species (for an initial AgNPs concentration of 1×10^{-5} to 1×10^{-4} M) were present in these two experiments (Figure 6). Despite similar soluble Ag species concentrations, the speciation differs. In the case of AgNPs aged in DI water, only Ag^+ can account for the soluble species. In contrast, the soluble Ag species predicted by equilibrium thermodynamics for AgNPs that aged in 0.5 M NaCl are $AgCl_2^-$, $AgCl_3^{2-}$, and $AgCl_4^{3-}$. Ligation by chlorine and differences in the total charge for soluble Ag species therefore does not appear to affect their toxicity to *E. coli*. However, this conclusion cannot be generalized to other organisms because toxicity can strongly depend on the route of exposure.[36]

Implications for Toxicity Studies and the Environment. The reaction of Cl^- with AgNPs has significant implications for the fate and effects of AgNPs in the environment. First, their reactions under different environmental conditions need to be carefully considered when assessing the toxicity of AgNPs. Even though the effects of the morphological and surface properties of AgNPs (i.e., size,[37] shape,[38] nature of the organic coating, and surface charge[39,40]) on toxicity have been studied, very few studies have looked carefully at the effect of inorganic ligands such as chloride on dissolution rate and toxicity. This is especially important because Cl^- is most often present in culture media used in toxicity studies. The amounts of chloride in those media can vary from almost no chloride to as high as 20−25 wt %[41−44]. The amount of chloride in solution will strongly affect the amount of soluble Ag present and will also potentially affect its toxicity. Thus, differences in chloride concentration make comparisons between toxicity studies performed in different media very difficult. As an example, we have recently shown that the same toxicity experiments run in two media with different Cl^- concentrations strongly affect the toxicity results.[44] In all cases, toxicity to *E. coli* was well correlated with Ag speciation in a chloride medium (i.e., toxicity was lower when AgCl was expected to precipitate). The effect of chloride on AgNP dissolution needs to be better characterized prior to and during bacterial toxicity experiments in order to be able to compare one study to another. In particular, the effect of the nature of the coating on the rate of release in presence of chloride is unknown.

On the basis of thermodynamics, the most probable chemical transformations that AgNPs will undergo in the environment once Ag(0) is oxidized to Ag(I) are sulfidation and reactions with chloride including soluble Ag−Cl complexes.[7] Although sulfidation of the Ag(I) in AgNPs has been observed and is expected in reducing environments, reactions of Ag(I) in AgNPs with chloride are likely to be an important chemical reaction to consider for aerobic systems. In the environment, the expected concentrations of AgNPs released are lower than the concentrations used in this study. Blaser et al. estimated that in the worst case scenarios the predicted environmental concentrations of AgNPs in rivers would be about 3 nM.[45] To further complicate matters, the relatively high concentrations of

dx.doi.org/10.1021/es400396f | Environ. Sci. Technol. 2013, 47, 5738−5745

Cl^- in rivers relative to the expected Ag concentrations is predicted to be high (Cl/Ag ratio in the 10^5 range) and can go up to 10^8 for seawater (considering a typical Cl^- concentration of 0.001 M for rivers and 0.5 M for seawater). Therefore, no solid AgCl is expected to form under these "natural" conditions. On the basis of the data presented in Figure 5, it is most likely that the formation of soluble $AgCl_x^{(x-1)-}$ (and therefore bioavailable) species will increase the dissolution rate of the oxidized exterior of the AgNPs in any environmental waters, enabling further oxidation and dissolution such that the lifetime of AgNPs will be short. However, other processes can affect the dissolution rate of AgNPs in the presence of Cl. Among the potential ligands that can strongly affect the behavior of the AgNPs, natural organic matter and in particular thiols and reduced sulfur groups present in natural organic matter appear to strongly bind to AgNPs and will potentially compete with inorganic ligands such as Cl^-.[46] The behavior of AgNPs in complex systems that include both organic and inorganic ligands needs to be further explored to better estimate the lifetime and effects of AgNPs in natural waters.

■ ASSOCIATED CONTENT

Supporting Information

Conversion from optical density to colony-forming unit (CFU) and the effect of aggregation on dissolution rates. This material is available free of charge via the Internet at http://pubs.acs.org.

■ AUTHOR INFORMATION

Corresponding Author

*E-mail: levard@cerege.fr.

Present Address

#Clément Levard: Centre Européen de Recherche et d'Enseignement des Géosciences de l'Environnement (CEREGE)/UMR 7330, Europole de l'Arbois−BP80, 13545 Aix en Provence CEDEX 04, France.

Notes

The authors declare no competing financial interest.

■ ACKNOWLEDGMENTS

This study was supported by the National Science Foundation (NSF) and the United States Environmental Protection Agency (EPA) under NSF Cooperative Agreement EF-0830093, Center for Environmental Implications of Nanotechnology (CEINT). Any opinions, findings, conclusions, or recommendations expressed in this material are those of the authors and do not necessarily reflect the views of the NSF or the EPA. This work has not been subjected to EPA review, and no official endorsement should be inferred.

■ REFERENCES

(1) Navarro, E.; Baun, A.; Behra, R.; Hartmann, N. B.; Filser, J.; Miao, A. J.; Quigg, A.; Santschi, P. H.; Sigg, L. Environmental behavior and ecotoxicity of engineered nanoparticles to algae, plants, and fungi. *Ecotoxicology* **2008**, *17* (5), 372−386.

(2) Marambio-Jones, C.; Hoek, E. M. V. A review of the antibacterial effects of silver nanomaterials and potential implications for human health and the environment. *J. Nanopart. Res.* **2010**, *12* (5), 1531−1551.

(3) Fabrega, J.; Luoma, S. N.; Tyler, C. R.; Galloway, T. S.; Lead, J. R. Silver nanoparticles: Behaviour and effects in the aquatic environment. *Environ. Int.* **2011**, *37* (2), 517−531.

(4) Panyala, N. R.; Pena-Mendez, E. M.; Havel, J. Silver or silver nanoparticles: a hazardous threat to the environment and human health? *J. Appl. Biomed.* **2008**, *6* (3), 117−129.

(5) Klaine, S. J.; Alvarez, P. J. J.; Batley, G. E.; Fernandes, T. F.; Handy, R. D.; Lyon, D. Y.; Mahendra, S.; McLaughlin, M. J.; Lead, J. R. Nanomaterials in the environment: Behavior, fate, bioavailability, and effects. *Environ. Toxicol. Chem.* **2008**, *27* (9), 1825−1851.

(6) Luoma, S. N. *Silver Nanotechnologies and the Environment: Old Problems or New Challenges*; The PEW Charitable Trusts: Washington, DC, 2008.

(7) Levard, C.; Hotze, E. M.; Lowry, G. V.; Brown, G. E. Environmental transformations of silver nanoparticles: Impact on stability and toxicity. *Environ. Sci. Technol.* **2012**, *46* (13), 6900−6914.

(8) Lowry, G. V.; Gregory, K. B.; Apte, S. C.; Lead, J. R. Transformations of nanomaterials in the environment. *Environ. Sci. Technol.* **2012**, *46* (13), 6893−6899.

(9) Lowry, G. V.; Espinasse, B. P.; Badireddy, A. R.; Richardson, C. J.; Reinsch, B. C.; Bryant, L. D.; Bone, A. J.; Deonarine, A.; Chae, S.; Therezien, M.; Colman, B. P.; Hsu-Kim, H.; Bernhardt, E. S.; Matson, C. W.; Wiesner, M. R. Long-term transformation and fate of manufactured Ag nanoparticles in a simulated large scale freshwater emergent wetland. *Environ. Sci. Technol.* **2012**, *46* (13), 7027−7036.

(10) Levard, C.; Reinsch, B. C.; Michel, F. M.; Oumahi, C.; Lowry, G. V.; Brown, G. E. J. Sulfidation processes of PVP-coated silver nanoparticles in aqueous solution: Impact on dissolution rate. *Environ. Sci. Technol.* **2011**, *45* (12), 5260−5266.

(11) Reinsch, B. C.; Levard, C.; Li, Z.; Ma, R.; Wise, A.; Gregory, K. B.; Brown, G. E., Jr.; Lowry, G. V. Sulfidation of silver nanoparticles decreases *Escherichia coli* growth inhibition. *Environ. Sci. Technol.* **2012**, *46* (13), 6992−7000.

(12) Cai, W.; Zhong, H.; Zhang, L. Optical measurements of oxidation behavior of silver nanometer particle within pores of silica host. *J. Appl. Phys.* **1998**, *83* (3), 1705−1710.

(13) Kim, B.; Park, C. S.; Murayama, M.; Hochella, M. F., Jr. Discovery and characterization of silver sulfide nanoparticles in final sewage sludge products. *Environ. Sci. Technol.* **2010**, *44* (19), 7509−7514.

(14) Kaegi, R.; Voegelin, A.; Sinnet, B.; Zuleeg, S.; Hagendorfer, H.; Burkhardt, M.; Siegrist, H. Behavior of metallic silver nanoparticles in a pilot wastewater treatment plant. *Environ. Sci. Technol.* **2011**, *45* (9), 3902−3908.

(15) Silver, S. Bacterial silver resistance: Molecular biology and uses and misuses of silver compounds. *FEMS Microbiol. Rev.* **2003**, *27* (2−3), 341−353.

(16) Nichols, J. W.; Brown, S.; Wood, C. A.; Walsh, P. J.; Playle, R. C. Influence of salinity and organic matter on silver accumulation in Gulf toadfish (*Opsanus beta*). *Aquat. Toxicol.* **2006**, *78* (3), 253−261.

(17) Gupta, A.; Maynes, M.; Silver, S. Effects of halides on plasmid-mediated silver resistance in *Escherichia coli*. *Appl. Environ. Microbiol.* **1998**, *64* (12), 5042−5045.

(18) Li, X.; Lenhart, J. J.; Walker, H. W. Dissolution-accompanied aggregation kinetics of silver nanoparticles. *Langmuir* **2010**, *26* (22), 16690−16698.

(19) Ho, C. M.; Yau, S. K. W.; Lok, C. N.; So, M. H.; Che, C. M. Oxidative dissolution of silver nanoparticles by biologically relevant oxidants: A kinetic and mechanistic study. *Chem.−Asian J.* **2010**, *5* (2), 285−293.

(20) Kim, D.; Jeong, S.; Moon, J. Synthesis of silver nanoparticles using the polyol process and the influence of precursor injection. *Nanotechnology* **2006**, *17*, 4019−4024.

(21) Ma, R.; Levard, C.; Marinakos, S. M.; Cheng, Y. W.; Liu, J.; Michel, F. M.; Brown, G. E.; Lowry, G. V. Size-controlled dissolution of organic-coated silver nanoparticles. *Environ. Sci. Technol.* **2012**, *46* (2), 752−759.

(22) Farkas, J.; Christian, P.; Gallego-Urrea, J. A.; Roos, N.; Hassellov, M.; Tollefsen, K. E.; Thomas, K. V. Uptake and effects of manufactured silver nanoparticles in rainbow trout (*Oncorhynchus mykiss*) gill cells. *Aquatic Toxicology* **2011**, *101* (1), 117−125.

(23) El Badawy, A. M.; Luxton, T. P.; Silva, R. G.; Scheckel, K. G.; Suidan, M. T.; Tolaymat, T. M. Impact of environmental conditions (pH, ionic strength, and electrolyte type) on the surface charge and aggregation of silver nanoparticles suspensions. *Environ. Sci. Technol.* **2010**, *44* (4), 1260−1266.
(24) Puigdomenech, I. *MEDUSA (Making Equilibrium Diagrams/ Using Sophisticated Algorithms)*; Royal Institute of Technology: Stockholm, 2004.
(25) Ha, H.; Payer, J. The effect of silver chloride formation on the kinetics of silver dissolution in chloride solution. *Electrochim. Acta* **2011**, *56* (7), 2781−2791.
(26) Yin, Y.; Li, Z. Y.; Zhong, Z.; Gates, B.; Xia, Y.; Venkateswaran, S. Synthesis and characterization of stable aqueous dispersions of silver nanoparticles through the Tollens process. *J. Mater. Chem.* **2002**, *12*, 522−527.
(27) Henglein, A. Colloidal silver nanoparticles: Photochemical preparation and interaction with O_2, CCl_4, and some metal ions. *Chem. Mater.* **1998**, *10* (1), 444−450.
(28) Chen, M.; Wang, L. Y.; Han, J. T.; Zhang, J. Y.; Li, Z. Y.; Qian, D. J. Preparation and study of polyacryamide-stabilized silver nanoparticles through a one-pot process. *J. Phys. Chem. B* **2006**, *110* (23), 11224−11231.
(29) Liu, J.; Hurt, R. H. Ion release kinetics and particle persistence in aqueous nano-silver colloids. *Environ. Sci. Technol.* **2010**, *44*, 2169−2175.
(30) Yin, L. Y.; Cheng, Y. W.; Espinasse, B.; Colman, B. P.; Auffan, M.; Wiesner, M.; Rose, J.; Liu, J.; Bernhardt, E. S. More than the ions: The effects of silver nanoparticles on *Lolium multiflorum*. *Environ. Sci. Technol.* **2011**, *45* (6), 2360−2367.
(31) Xiu, Z.-m.; Zhang, Q.-b.; Puppala, H. L.; Colvin, V. L.; Alvarez, P. J. J. Negligible particle-specific antibacterial activity of silver nanoparticles. *Nano Lett.* **2012**, *12* (8), 4271−4275.
(32) Xiu, Z.-M.; Ma, J.; Alvarez, P. J. J. Differential effect of common ligands and molecular oxygen on antimicrobial activity of silver nanoparticles versus silver ions. *Environ. Sci. Technol.* **2011**, *45* (20), 9003−9008.
(33) Sotiriou, G. A.; Pratsinis, S. E. Antibacterial activity of nanosilver ions and particles. *Environ. Sci. Technol.* **2010**, *44* (14), 5649−5654.
(34) Lubick, N. Nanosilver toxicity: Ions, nanoparticies, or both? *Environ. Sci. Technol.* **2008**, *42* (23), 8617−8617.
(35) Fabrega, J.; Fawcett, S. R.; Renshaw, J. C.; Lead, J. R. Silver nanoparticle impact on bacterial growth: Effect of pH, concentration, and organic matter. *Environ. Sci. Technol.* **2009**, *43* (19), 7285−7290.
(36) Bielmyer, G. K.; Brix, K. V.; Grosell, A. Is Cl-protection against silver toxicity due to chemical speciation? *Aquat. Toxicol.* **2008**, *87* (2), 81−87.
(37) Choi, O.; Hu, Z. Q. Size dependent and reactive oxygen species related nanosilver toxicity to nitrifying bacteria. *Environ. Sci. Technol.* **2008**, *42* (12), 4583−4588.
(38) Pal, S.; Tak, Y. K.; Song, J. M. Does the antibacterial activity of silver nanoparticles depend on the shape of the nanoparticle? A study of the gram-negative bacterium *Escherichia coli*. *Appl. Environ. Microbiol.* **2007**, *73* (6), 1712−1720.
(39) Shoults-Wilson, W. A.; Reinsch, B. C.; Tsyusko, O. V.; Bertsch, P. M.; Lowry, G. V.; Unrine, J. M. Effect of silver nanoparticle surface coating on bioaccumulation and reproductive toxicity in earthworms (*Eisenia fetida*). *Nanotoxicology* **2011**, *5* (3), 432−444.
(40) El Badawy, A. M.; Silva, R. G.; Morris, B.; Scheckel, K. G.; Suidan, M. T.; Tolaymat, T. M. Surface charge-dependent toxicity of silver nanoparticles. *Environ. Sci. Technol.* **2011**, *45* (1), 283−287.
(41) Sinha, R.; Karan, R.; Sinha, A.; Khare, S. K. Interaction and nanotoxic effect of ZnO and Ag nanoparticles on mesophilic and halophilic bacterial cells. *Bioresour. Technol.* **2011**, *102* (2), 1516−1520.
(42) Meyer, J. N.; Lord, C. A.; Yang, X. Y. Y.; Turner, E. A.; Badireddy, A. R.; Marinakos, S. M.; Chilkoti, A.; Wiesner, M. R.; Auffan, M. Intracellular uptake and associated toxicity of silver nanoparticles in *Caenorhabditis elegans*. *Aquat. Toxicol.* **2010**, *100* (2), 140−150.
(43) Hedi, A.; Sadfi, N.; Fardeau, M.-L.; Rebib, H.; Cayol, J.-L.; Ollivier, B.; Boudabous, A. Studies on the biodiversity of halophilic microorganisms isolated from El-Djerid salt lake (Tunisia) under aerobic conditions. *Int. J. Microbiol.* **2009**, *2009*, 731786.
(44) Levard, C.; Hotze, E. M.; Colman, B. P.; Truong, L.; Yang, X. Y.; Bone, A.; Brown, G. E. J.; Tanguay, R. L.; Di Giulio, R. T.; Bernhardt, E. S.; Meyer, J. N.; Wiesner, M.; Lowry, G. V. Sulfidation of AgNPs: A natural antidote to their toxicity for a diverse range of organisms. *ACS Nano* **2013**, submitted.
(45) Blaser, S. A.; Scheringer, M.; MacLeod, M.; Hungerbuhler, K. Estimation of cumulative aquatic exposure and risk due to silver: Contribution of nano-functionalized plastics and textiles. *Sci. Total Environ.* **2008**, *390* (2−3), 396−409.
(46) Gondikas, A. P.; Morris, A.; Reinsch, B. C.; Marinakos, S. M.; Lowry, G. V.; Hsu-Kim, H. Cysteine-induced modifications of zero-valent silver nanomaterials: Implications for particle surface chemistry, aggregation, dissolution, and silver speciation. *Environ. Sci. Technol.* **2012**, *46* (13), 7037−7045.